

Fission of $^{228}\text{Ra}^\dagger$

J. Weber,* H. C. Britt, A. Gavron,[‡] E. Konecny,[§] and J. B. Wilhelmy
Los Alamos Scientific Laboratory, University of California, Los Alamos, New Mexico, 87545
 (Received 26 January 1976)

Fission probabilities and mass distribution have been measured as a function of excitation energy for ^{228}Ra excited in the $^{226}\text{Ra}(t, pf)$ reaction. Triple peaked mass distributions are observed for which the symmetric component has an apparent higher threshold by over 1 MeV. Results are analyzed in a statistical model which suggests the presence of a resonance in the fission probability for the asymmetric mass component and the need for level density enhancements (possibly due to axial asymmetry at the barrier) in the analysis of the fission probability for the symmetric component.

[NUCLEAR REACTIONS, FISSION $^{226}\text{Ra}(t, pf)$; measured fission probabilities
 for symmetric and asymmetric components; deduced fission barrier param-
 eters, fission mass distributions.]

I. INTRODUCTION

The most striking experimental feature of the fission of nuclei in the "Ra region" is the simultaneous occurrence of symmetric and asymmetric components in the mass distribution.¹⁻⁴ Recent direct reaction experiments⁵ of the type $^{226}\text{Ra}(\text{}^3\text{He}, xf)$ (where $x = p, d, t, \alpha$) have yielded two important features:

(1) The symmetric and asymmetric mass components occur in the fission of a single isotope at well defined excitation energies and are therefore not the result of a mixture of possible symmetric and asymmetric components in adjacent isotopes produced by first and second chance fission competition.

(2) For ^{227}Ac and ^{228}Ac the symmetric and asymmetric components are shown to be associated with different thresholds. This indicates that for these nuclei the decision on whether fission proceeds via the resolved symmetric or asymmetric components is strongly influenced in the region of the saddle point; it cannot be simply a property of static and/or dynamic effects in the region of the scission point.

Theoretical developments which use the Strutinskii method for calculating potential energy surfaces and include octopole deformations have shown that the second (outer) saddle point for the actinide nuclei favor reflection asymmetric shapes.⁶⁻⁹ This has been interpreted as being a major cause for the observed asymmetric fission of the actinide nuclei. In the Ra region the triple peaked mass distributions are more difficult to explain. The calculations predict a reflection asymmetric saddle point for these nuclei (as they do for the heavier actinides), with a low first barrier that is not expected to influence the fission

process. It is therefore difficult to understand why the mass distribution in these isotopes should exhibit both symmetric and asymmetric components from an analysis of the saddle points of the published potential energy surfaces.

Since the theoretical calculations that have been published are for even-even nuclei and the recent direct reaction data have been for odd- A and odd-odd nuclei, the apparent inconsistencies could possibly result from odd particle effects. To eliminate this possibility we felt that it was desirable to study the fission of an even-even nucleus formed by bombardment of an even-even target. The only convenient target available in this region is the 1600-yr ^{226}Ra . In this paper we present fission probability distributions for symmetric and asymmetric components from the $^{226}\text{Ra}(t, pf)$ reaction.

Analysis of the experimental data show that the fission barrier is far more complex than is evident in published potential energy surface calculations. There is reason to believe that in the mass asymmetric surface there are two barriers of approximately equal height. In the mass symmetric surface, a large level density enhancement factor is necessary to fit the fission probability. This could mean that the second barrier involved in symmetric fission is axially deformed.

II. EXPERIMENTAL ARRANGEMENT AND DATA REDUCTION

A 23 MeV tritium beam was supplied by the three-stage Van de Graaff facility at the Los Alamos Scientific Laboratory and used to bombard a $75 \mu\text{g}/\text{cm}^2$ ^{226}Ra target which had been vacuum evaporated onto a $30 \mu\text{g}/\text{cm}^2$ C foil. Data were obtained during two separate runs¹⁰ representing

approximately 80 and 100 beam hours. In the second run an improvement in detection solid angle was obtained and therefore it was possible to have a lower beam current (~ 90 nA as compared to ~ 130 nA in the first run) and still obtain acceptable counting rates (~ 1 identified coincident fission event per minute). This lowering of the beam intensity resulted in a decrease of the accidental coincidence yield from a total accidental to true ratio of 0.295 in the first run to a value of 0.136 in the second and thus resulted in improved sensitivity.

The experimental configuration for the second run is shown in Fig. 1. The outgoing protons from the direct reaction $^{226}\text{Ra}(t, p)^{228}\text{Ra}^*$ were identified and had their energy measured using a ΔE - E solid state counter telescope which was located at 95° with respect to the beam axis. From the known Q value and kinematics of the reaction it was then

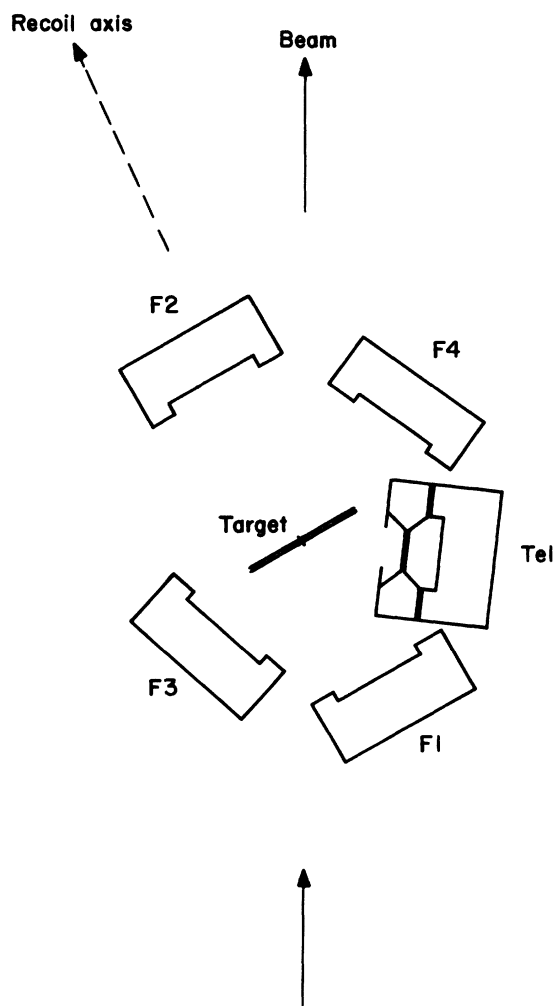


FIG. 1. Diagram of the experimental setup.

possible to convert the measured proton energies to excitation energies in the residual ^{228}Ra nucleus. The fission fragments were measured in coincidence with particle signals from the counter telescope in two pairs of 300 mm^2 solid state surface barrier heavy ion detectors which were located at $\sim 0^\circ$ and 90° relative to the recoil axis of the ^{228}Ra reaction product. The telescope was covered with a $60\text{ }\mu\text{m}$ Al foil which was used to prevent the α particles from the decay of the ^{226}Ra target material from reaching the ΔE detector. The electronic system utilized standard fast-slow coincidence logic with the fast signals being generated from constant fraction discriminators and pileup rejection being employed in the telescope circuit. The timing gate for the proton fission coincidence was ~ 1.3 ns. The digitized pulses were stored event by event using an on-line SDS 930 computer which also provided for monitoring control and data inspection. The stored events were sequentially written on magnetic tape for eventual off-line analysis.

The fission detectors were calibrated using a ^{252}Cf spontaneous fission source. The calibration procedure was repeated frequently during the course of the experiment in order to measure possible pulse height changes in the detector response caused by radiation damage. The proton energy calibration for the counter telescope was obtained using the $^{208}\text{Pb}(t, p)^{210}\text{Pb}^*$ reaction to the known levels of ^{210}Pb . The measured energy resolution for protons was ~ 200 keV.

The data were processed into three event types, each as a function of the excitation energy in ^{228}Ra . Event type (1) consisted of ΔE - E counter telescope coincidences which gave the proton spectrum [$^{226}\text{Ra}(t, p)^{228}\text{Ra}^*$ + contaminants; Fig. 2(c)] and was used to obtain the probability for leaving the $^{228}\text{Ra}^*$ at any specific excitation energy. Events of type (2) were coincidences between the counter telescope and one of the fission fragment detectors F1 or F3 (the closer of the two fission fragment detectors at 0° and 90° , respectively.) These events were used to extract the fission probability $P_f = \Gamma_f / \Gamma_{\text{tot}}$ [Figs. 2(a) and 2(b)]. Events of type (3) were coincidences between the counter telescope and two fission fragment detectors (either F1-F2 or F3-F4). For these events fission fragment mass analysis was performed using the correlated pulse heights of the two complementary detectors, the Schmitt procedure¹¹ for pulse height defect correction, mass and momentum conservation, and a correction for prompt neutron emission.¹² The extracted mass spectra for the total measured ^{228}Ra excitation energy range (7-13 MeV) and for the 7.00-8.85 MeV excitation increment are shown in Fig. 3.

The prompt coincidence timing data were stored in a spectral display which recorded the digitized output of a time-to-amplitude converter (TAC) that was started with a fission fragment and stopped with a suitably delayed pulse from the ΔE detector. This arrangement permitted a simple correction for the background chance coincidence events. The constant background in the TAC spec-

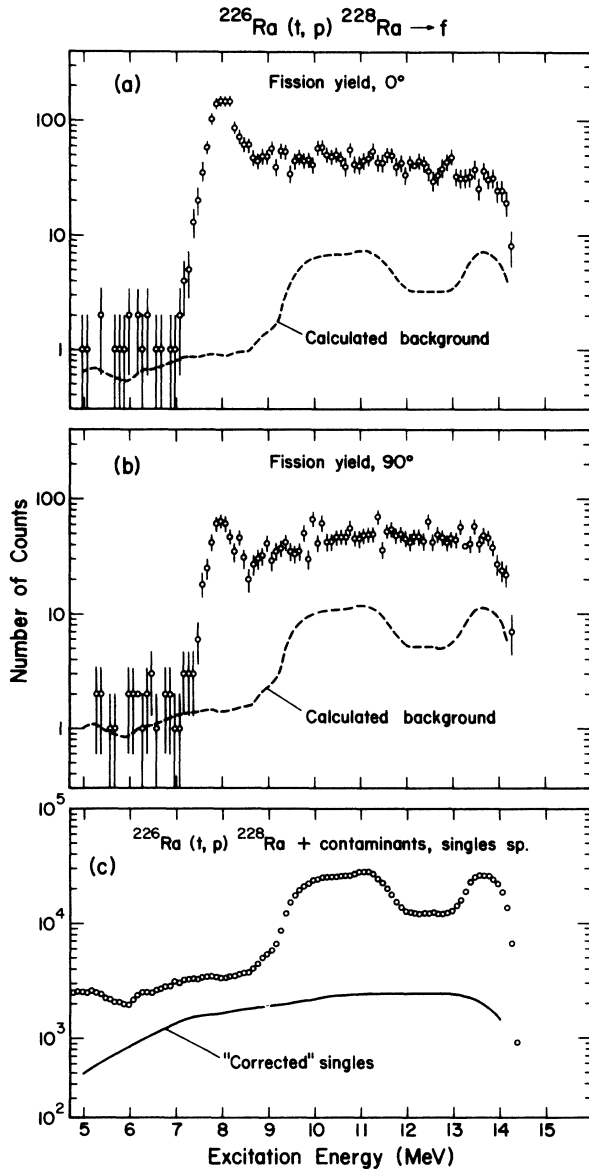


FIG. 2. (a) Fission yield of the 0° fission detector in the second run. (b) Fission yield of the 90° fission detector in the second run. (c) Open circles: Singles spectrum of the reaction $^{226}\text{Ra}(t, p)^{228}\text{Ra} + \text{contaminants}$ in the second run. Full line: Singles spectrum corrected for the contaminant contribution (correction described in the text).

trum gave the probability for a chance event. These chance events were assumed to have the same spectral distribution as the singles data [Fig. 2(c)] and could be appropriately subtracted from the measured coincidence data to give the true distribution. From these corrected data the fission probabilities and anisotropies [$\sigma_{\text{fiss}}(0^\circ)/\sigma_{\text{fiss}}(90^\circ)$] were calculated. The fission probabilities were obtained assuming a $P_2(\cos\theta)$ form for the angular correlation. Due to the large experimental solid angle the $^{226}\text{Ra}(t, p)^{228}\text{Ra}^*$ singles spectrum was obscured by broad carbon and oxygen contaminant peaks which were caused by reactions on the carbon backing and oxide of the target. To generate a "corrected" singles spectrum we measured the fission yield as a function of excitation energy for the reaction $^{231}\text{Pa}(t, pf)$ (using the same geometry and beam energy as the Ra experiment). The fission probability for ^{233}Pa is known¹³ up to excitation energies of 11 MeV. By assuming the fission probability was constant and equal to the value at 11 MeV for $E^* > 11$ MeV the singles spectrum for $^{231}\text{Pa}(t, p)^{233}\text{Pa}$ could then be extracted from the known data:

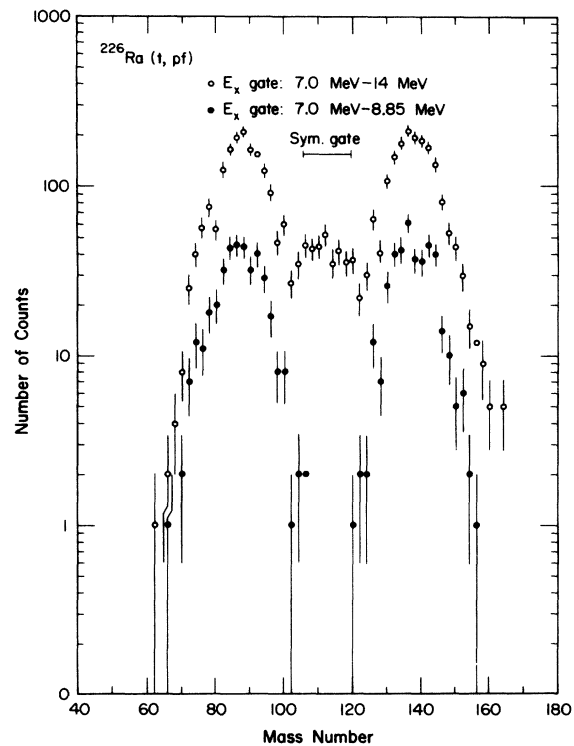


FIG. 3. Open circles: Mass spectrum of the reaction $^{226}\text{Ra}(t, pf)$ obtained in the 0° detector pair during the second run summed over the excitation energies $7 \text{ MeV} \leq E_x \leq 14 \text{ MeV}$. Full circles: Mass spectrum summed over excitation energies $7 \text{ MeV} \leq E_x \leq 8.85 \text{ MeV}$ (inter-threshold range).

$$\sigma_{(t,p)}(E^*, {}^{233}\text{Pa}) = \frac{\sigma_{f1ss}(E^*, {}^{233}\text{Pa})}{P_f(E^*, {}^{233}\text{Pa})}.$$

For excitation energies $E^* > 6$ MeV there should be no essential difference between the reaction ${}^{231}\text{Pa}(t,p){}^{233}\text{Pa}$ and ${}^{226}\text{Ra}(t,p){}^{228}\text{Ra}$ and therefore the extracted "singles" spectrum for the population of excited states in ${}^{233}\text{Pa}$ was also used for the evaluation of the fission probability of ${}^{228}\text{Ra}$ (except for a slight correction due to the different Coulomb barriers). Fission probabilities and fragment anisotropies were evaluated for both the events having a single measured fission fragment in coincidence with the protons in the counter telescope (type 2 events) and for the symmetric and asymmetric components of the mass distribution as calculated from the kinetic energies of the detected binary fission events in coincidence with protons (type 3 events). To obtain the fission probability for the symmetric mass division component the counts in the symmetric mass gate (Fig. 3) were multiplied by a scale factor transforming the area in the gate to an area corresponding to a symmetric mass distribution having a Gaussian shape with $\sigma = 12$ amu.³

III. RESULTS

The mass distribution for ${}^{228}\text{Ra}$ summed over the excitation energy range ($7 \text{ MeV} \leq E_x \leq 14 \text{ MeV}$) is shown in Fig. 3 (open circles). A triple humped shape is obtained with distinct minima between the peaks. This conclusively demonstrates (since second chance fission is energetically most improbable) that symmetric and asymmetric fission occur in the same even-even nucleus. Similar results were also found for the fission of the odd- A nucleus ${}^{227}\text{Ac}$ and odd-odd ${}^{228}\text{Ac}$.⁵

The fission probabilities and fragment anisotropies which were obtained from summing both experimental runs are presented in Fig. 4 as a function of excitation energy in ${}^{228}\text{Ra}$ for the total fission yield (open circles, no mass gate) and for the symmetric fission component (closed circles).¹⁴ The total fission probability begins to rise at $E^* \sim 7$ MeV, reaches a peak of $P_f = 2.6 \times 10^{-3}$ (at $E^* \sim 8$ MeV) and then drops at higher E^* to an approximately constant value of $P_f = 0.8 \times 10^{-3}$. The symmetric fission probability, however, is very low for $7 \text{ MeV} \leq E_x \leq 8.85 \text{ MeV}$ and starts to rise only at ~ 9 MeV. The symmetric fission yield in the 7–8.85 MeV energy range is consistent with zero and has, from analysis of the second more sensitive Ra experiment, an upper limit relative to the symmetric yield above 9 MeV (averaged from 9–10.85 MeV) of less than 4% with a 95% confidence level. This strongly suggests that in the fission of the even-even nucleus

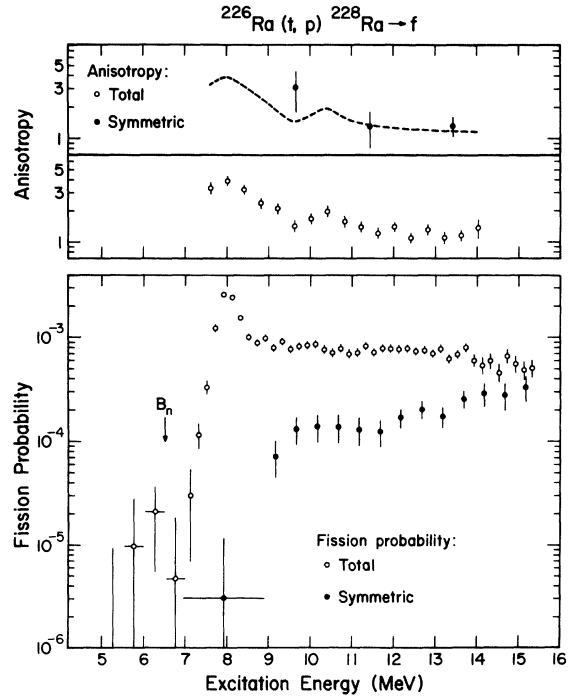


FIG. 4. Fission probabilities and fragment anisotropies as a function of excitation energy in the fissioning nucleus ${}^{228}\text{Ra}$, separately for total (○) and symmetric (●) fission. The approximate total anisotropy is repeated as a dashed line in the field of the symmetric anisotropy.

${}^{228}\text{Ra}$ symmetric and asymmetric fission are associated with different thresholds.

Near threshold large anisotropies are found due to the population primarily of the lowest $K = 0$ bands. As the excitation energy is increased additional K states can contribute to the total fission probability and the anisotropy is decreased.¹⁵ The symmetric yield also seems to exhibit this type of behavior though not as clearly because of the poorer statistical accuracy.

The ratio $P_f(\text{sym})/P_f(\text{asym})$ as a function of excitation is presented in Fig. 5. The important point in this figure is that at excitation energies greater than 14.5 MeV the yield of symmetric fission has crossed the yield of asymmetric fission and has become the dominant component. A similar situation occurs in ${}^{227,228}\text{Ac}$,⁵ however, in those cases the "crossing point" was above the threshold for second chance fission and had to be extrapolated from the first chance fission trends.

IV. THEORETICAL ANALYSIS AND DISCUSSION

We have attempted to analyze the asymmetric and symmetric fission probabilities within the framework of previously developed statistical models,^{13,16} and for this discussion will separate the analysis in two parts: (1) the mass asymmetric com-

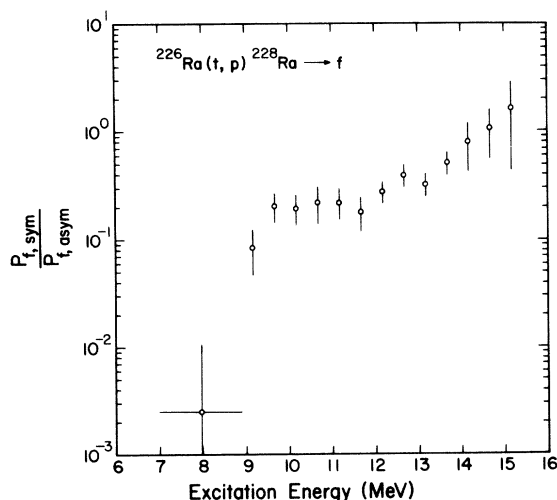


FIG. 5. $P_{f,sym}/P_{f,asym}$ as a function of excitation energy in the fissioning nucleus ^{228}Ra .

ponent (which for low excitation energies is equivalent to the total fission probability) and (2) the mass symmetric component.

A. Asymmetric component

Using a statistical model which includes possible enhancement effects,¹³ and assuming the first barrier to be axially symmetric and the second to be mass asymmetric, we obtain the best fit using barrier parameters listed in Table I. The results of this analysis are shown as the solid line in Fig. 6. While there is reasonable agreement between the calculated and experimental fission probabilities well above the barrier, the model is not able to reproduce the narrow peak around 8 MeV. The model assumes there are no additional band heads

TABLE I. Fission barrier parameters obtained from fits to the experimental data as described in the text. Uncertainties in the barrier heights are $\sim \pm 0.3$ MeV for the highest of the two peaks within the framework of the models used for analysis. Uncertainties in the heights of the lower of the two peaks can be somewhat greater and for the nonresonant analysis are dependent on the absolute normalization of the fission probabilities. The two barriers can be interchanged without affecting the results. All units are in MeV.

	E_a	E_2	E_b	$\hbar\omega_a$	$\hbar\omega_2$	$\hbar\omega_b$
Asymmetric component						
Nonresonant	7.8	...	8.9	1.6	...	0.5
Resonant	8.2	7.1	8.2	2.0	2.1	2.0
Symmetric component						
Axial symmetric	7.5	...	9.1	0.7	...	0.5
Axial asymmetric	<7.5	...	9.3	0.7

between 8.0–9.0 MeV and the drop in the calculated fission probability above 8.0 MeV is due to neutron competition with the first spin-0 fission channels and their rotational bands. Therefore, with this model which uses nonresonant penetration through the two barriers (i.e., complete mixing in the second well), there is no method to obtain a more narrow peak. It is evident that the observed narrow peak can only be reproduced by attempting to analyze it as a transmission resonance. Using such a resonant penetration model¹⁶ which has been modified to include neutron competition, we obtain a much improved fit (the dashed line in Fig. 6). This model, which uses discrete channels, is only applicable in the region near the fission barriers where the level density has not become excessively large. The extracted barrier parameters are listed in Table I (E_2 and $\hbar\omega_2$ are the height and curvature of the second minimum).

From this analysis we conclude there is reasonable evidence that the peak in the fission probability at 8.0 MeV is caused by a transmission resonance. Even if this is not a resonance, both models predict that the two fission barriers are of comparable size. This is contrary to existing theo-

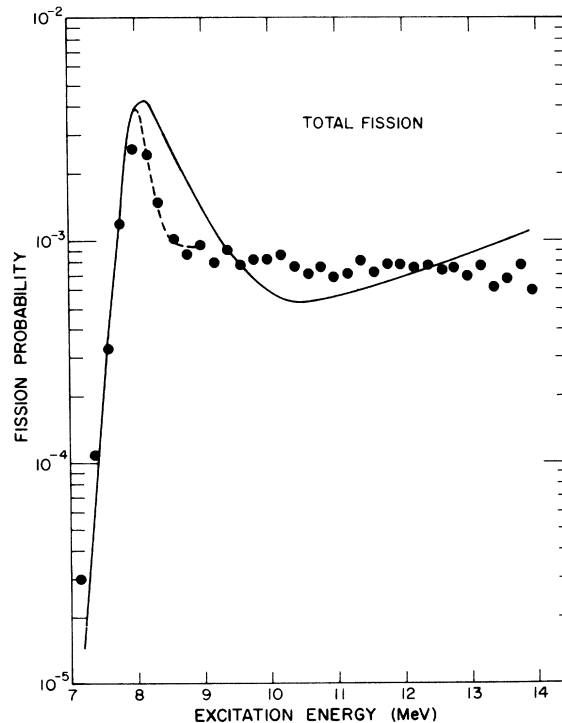


FIG. 6. Model analysis of the total fission probability. The full line is the calculated asymmetric yield plus the experimental symmetric yield and describes the fit obtained assuming a double humped barrier with complete mixing in the second well. The dashed line describes resonant penetration in the barrier region.

retical calculations in which a very low first barrier is predicted.⁶⁻⁹ It is possible that we are observing the effects of a triple peaked fission barrier. In this case the second broad barrier has split into two parts whereas the (calculated) first barrier is indeed too low to have significant effect on the fission probability. Such an effect has been suggested by Moller and Nix¹⁷ to explain the "thorium anomaly" in which transmission resonances are observed for isotopes where theoretically the two peaks of the fission barrier are predicted to be substantially different.

B. Symmetric component

The initial analysis of the symmetric fission probability was made assuming the contributing second barrier was mass (reflection) and axially symmetric. The results of this analysis are shown as a full line in Fig. 7 where the best extracted barrier parameters are listed in Table I. The calculated fission probability overestimates the experimental value at the barrier but then decreases to a value ~ 5 times lower than the experimental probability. The fission probability is being limited by the number of levels available

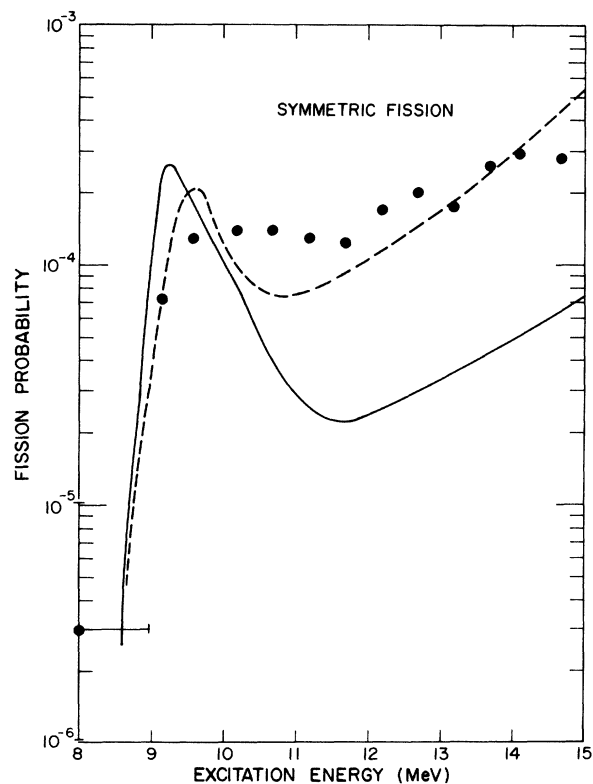


FIG. 7. Model analysis of the mass symmetric fission probability: the full line assumes an axially symmetric second barrier, and the dashed line a γ deformed one.

above the second barrier. The number of levels could be increased by decreasing the height of the second barrier but this would only result in large discrepancies with the symmetric fission threshold. This situation is similar to what we had previously encountered in actinide fission where the fission probability was being limited by levels above the first barrier.¹³ The solution to that problem, and also apparently for our symmetric Ra fission, is that a large enhancement to the level density is necessary to fit the experimental results. Such an enhancement can occur by having an axially asymmetric shape at the saddle point. Very recent calculations by Larsson¹⁸ indicate that the second symmetric barrier in ²²⁸Ra is quite soft with respect to axial asymmetric (γ) deformations. He finds a shell + pairing energy gain of 6 MeV for γ deformations of 20° at the ϵ_1, ϵ_4 (0.90, 0.12) coordinates which correspond approximately to the ²²⁸Ra symmetric saddle point. Some 5 MeV of this gain is compensated for by the increase in the liquid drop portion of the potential energy surface at this γ deformation. If we use these results and assume the second, reflection symmetric, fission barrier in Ra to be axially deformed (*R* point group symmetry¹³), we obtain the fit shown as the dashed line in Fig. 7 barrier parameters given in Table I. Though enhancement effects are essential to obtain a good fit to the data, we are not yet in a position to unequivocally imply that the second barrier is axially asymmetric. Other enhancement effects such as low lying vibrations or even possibly dynamical considerations (though these appear less likely since there is such a sharp drop in symmetric fission probability below 9 MeV) could contribute to the observed phenomena. We note also that the first barrier is essentially undetermined in this analysis: the fission probability is controlled entirely by the second barrier.

It is worth remarking that the required enhancement effects cannot be obtained by reasonable variations in the calculated intrinsic level densities. We have found that even by varying between single particle levels appropriate to shell and antishell regions, the calculated level densities (which include pairing) differ by no more than a factor of 2 at excitation energies below 10 MeV. The required enhancement factor to fit the data is of the order of 5-15 (depending on E_x). Enhancement effects in the symmetric fission component also seem to be required for other fissioning nuclei in this region. We have been able to obtain adequate fits to the published⁵ actinium fission data only by assuming axial asymmetry in those nuclei at the second mass reflection symmetric barrier.

An additional comment about the implication of

different thresholds for asymmetric and symmetric mass division should be made. Since our extraction of the fission barrier properties is in such large discrepancy with any published theoretical prediction it is not appropriate to make a detailed comparison of predicted saddle point properties with the observed mass distribution. However, the occurrence of significant amounts of symmetric and asymmetric fission components, even though they have substantially different thresholds (from our analysis a difference of over 1 MeV between asymmetric and symmetric fission), is contrary to the spirit of the analysis of Pauli⁷ in which he infers significant yields of the two components only when the thresholds are quite similar. Also, the existence of different fission thresholds means the system must make the qualitative decision between symmetric and asymmetric fission at the saddle point and (at least for this aspect of fission) not be dominated by the potential energy surface closer to scission.

V. CONCLUSION

In conclusion the experimental data have shown: (1) Triple peaked fission mass distributions occur in first chance fission of even-even nuclei. (2) There is an apparent different threshold for asymmetric and symmetric fission. (3) Once above threshold the symmetric fission increases more

rapidly than the asymmetric and eventually becomes the dominant component.

From our analysis of the fission probability we conclude: (1) There is reasonable evidence that the peak in the fission probability at 8.0 MeV is caused by a transmission resonance. (2) This resonance is qualitatively consistent with the hypothesis that the asymmetric outer barrier may have split into two components which would result in a triple peaked fission barrier. (3) The symmetric second barrier requires a large enhancement factor which may be due to an axially asymmetric shape. From the evidence for resonance phenomena and level density enhancement we conclude that the potential energy surfaces in the vicinity of the fission barriers of the Ra region nuclei are much more complicated than published theoretical predictions.

ACKNOWLEDGMENTS

It is a pleasure to acknowledge very useful discussions on the interpretation of these results with A. Bohr, A. Kerman, P. Möller, S. G. Nilsson, and J. R. Nix. We would like to thank S. E. Larsson and S. G. Nilsson for calculating potential energy surfaces for the γ asymmetric regions near the symmetric saddle point and communicating the results to us.

†Work supported by the U. S. Energy Research and Development Administration.

*Current address: Universität München, München, West Germany.

‡On leave of absence from the Weizmann Institute of Science, Rehovot, Israel.

§Current address: Drägerwerk, Postfach 1339, 24 Lübeck 1, West Germany.

¹R. C. Jensen and A. W. Fairhall, Phys. Rev. **109**, 942 (1958); **118**, 771 (1960).

²H. C. Britt, H. E. Wegner, and J. C. Gursky, Phys. Rev. **129**, 2239 (1963); H. C. Britt and S. L. Whetstone, *ibid.* **133**, B603 (1964).

³E. Konecny and H. W. Schmitt, Phys. Rev. **172**, 1213, 1226 (1968).

⁴D. G. Perry and A. W. Fairhall, Phys. Rev. C **4**, 977 (1971).

⁵E. Konecny, H. J. Specht, and J. Weber, Phys. Lett. **45B**, 329 (1973); and in *Proceedings of the Third International Atomic Energy Symposium on Physics and Chemistry of Fission, Rochester, New York, 1973* (International Atomic Energy Agency, Vienna, 1974), Vol. II, p. 3.

⁶P. Möller, Nucl. Phys. **A192**, 529 (1972).

⁷H. C. Pauli, Phys. Rep. **7C**, 35 (1973).

⁸M. Bolsterli, E. O. Fiset, J. R. Nix, and J. L. Norton, Phys. Rev. C **5**, 1050 (1972).

⁹M. G. Mustafa, U. Mosel, and H. W. Schmitt, Phys. Rev. C **7**, 1519 (1973).

¹⁰The excitation energy range covered in the first run was $5 \text{ MeV} \leq E^* \leq 16 \text{ MeV}$; in the second run, $3 \text{ MeV} \leq E^* \leq 14 \text{ MeV}$.

¹¹H. W. Schmitt, W. E. Kiker, and C. W. Williams, Phys. Rev. **137**, B837 (1965).

¹²E. Konecny (unpublished).

¹³A. Gavron, H. C. Britt, E. Konecny, J. Weber, and J. B. Wilhelmy, Phys. Rev. Lett. **34**, 827 (1975).

¹⁴The data for the two runs were averaged with statistical weight as follows:

$$P_f = \frac{W_{\text{run } 1} P_{f, \text{run } 1} + W_{\text{run } 2} P_{f, \text{run } 2}}{W_{\text{run } 1} + W_{\text{run } 2}},$$

where $W = 1/\sigma^2$.

¹⁵J. D. Cramer and H. C. Britt, Phys. Rev. C **2**, 2350 (1970).

¹⁶B. B. Back, O. Hansen, H. C. Britt, and J. D. Garrett, Phys. Rev. C **9**, 1924 (1974).

¹⁷P. Moller and J. R. Nix, in *Proceedings of the Third International Atomic Energy Symposium on Physics*

and Chemistry of Fission, Rochester, New York, 1973
(see Ref. 5), Vol. I, p. 103.

¹⁸S. E. Larsson (private communication). See for similar
calculations S. E. Larsson and G. Leander, in *Proceed-*

ings of the Third International Atomic Energy Symposi-
um on Physics and Chemistry of Fission, Rochester,
New York, 1973 (see Ref. 5), Vol. I, p. 177.